CHEMISTRY
A EUROPEAN JOURNAL

DOI: 10.1002/chem.200902839

Spermine-Functionalized Perylene Bisimide Dyes—Highly Fluorescent Bola-Amphiphiles in Water

Stefanie Rehm, Vladimir Stepanenko, Xin Zhang, Thomas H. Rehm, and Frank Würthner*[a]

Dedicated to Professor Franz Effenberger on the occasion of his 80th birthday

Abstract: A series of four spermine-functionalized perylene bisimide dyes without linkers (**1**) and with linkers (**2**–**4**) between the chromophore and the polyamine was synthesized. Protonation of the spermine moieties resulted in the formation of highly water-soluble dyes with up to six positively charged ammonium ions. The aggregation behavior of these strongly fluorescent bola-amphiphiles was studied in pure water as solvent by UV/Vis and fluorescence spectroscopy, and an astonishingly high fluorescence quantum yield of up to $\Phi_{fl} = 0.90$ was observed for PBI **1**. Atomic force microscopy and transmission electron microscopy were applied for the visualization of the aggregates on surfaces. Molecular modeling studies were performed by force-field calculations to explore the aggregate morphologies, which also provided valuable information on the influence of the additional alkylcarbonyl linkers. Our detailed spectroscopic and microscopic investigations revealed that the excellent optical properties of perylene bisimide chromophores can be used even in pure deionized water if their aggregation is efficiently suppressed.

Keywords: aggregation · dyes/pigments · fluorescence · perylene · spermine · water chemistry

Introduction

In the past years, perylenetetracarboxylic acid bisimides (PBIs) evolved as one of the most intensively studied classes of functional dyes. Their outstanding optical and redox properties in combination with their thermal and light stability give rise to applications in different fields of current research. PBIs were initially used as high-performance pigments on industrial scale due to their wide color range in the solid state and their extremely low solubility.[1] The latter property prevented the use of PBIs in solution and their targeted derivatization. Through the introduction of solubility-enhancing groups, such as alkyl chains at the imide and bay position of the PBI, it was possible to overcome their low solubility and investigate the optical properties of molecular dyes as strong fluorophores as well as their aggregation behavior as novel supramolecular building blocks.[2] As a result of this development, PBIs are nowadays widely used as fluorophores in organic media,[3] as organic semiconductors in solar cells,[4] as light-emitting diodes[5] and field effect transistors,[6] as π-acidic anion receptors,[7] or as high-performance fluorophores for protein labeling[8] and DNA research.[9]

However, upon changing the focus from common organic solvents to the biologically most relevant solvent water, new strategies for the synthesis of PBI dyes have to be developed, because the solubility of the chromophore decreases rapidly with the increasing polarity of the solvent.[10] Uncharged residues such as polyethylene glycol chains,[11] hydrophilic dendrimers,[12] crown ethers[13] and cyclodextrins,[14] as well as peptide chains[15] have been employed for the solubilization of the perylene core. These systems could be used, for instance, as biocompatible and biodegradable staining materials for cells,[16] or, for example, as guanine-quadruplex-inducing DNA intercalators.[17] Nevertheless, most of these PBIs are not highly soluble in pure water or

[a] Dipl.-Chem. S. Rehm, Dr. V. Stepanenko, Dr. X. Zhang, Dr. T. H. Rehm, Prof. Dr. F. Würthner
Institut für Organische Chemie, Universität Würzburg
Am Hubland, 97074 Würzburg (Germany)
Fax: (+49) 931-31-84756
E-mail: wuerthner@chemie.uni-wuerzburg.de

Supporting information for this article is available on the WWW under http://dx.doi.org/10.1002/chem.200902839.

exhibit unfavorable fluorescence properties due to aggregate formation.[18] To address these deficiencies, charged groups, either permanent ions or reversible ionic groups were introduced by protonation and deprotonation. For anionic derivatives of water-soluble PBIs, carboxylate and sulfonate groups have most often been incorporated through the phenoxy substituents in the bay region.[19] In addition, permanent positive charges were created at the imide position by alkylation of amino groups or nitrogen-containing heterocycles.[20] The combination of the excellent optical properties of the PBI chromophore with the strongly enhanced water solubility have been used for single-molecule spectroscopy of biological systems, for example, for tracking experiments of bioparticles in living cells.[21]

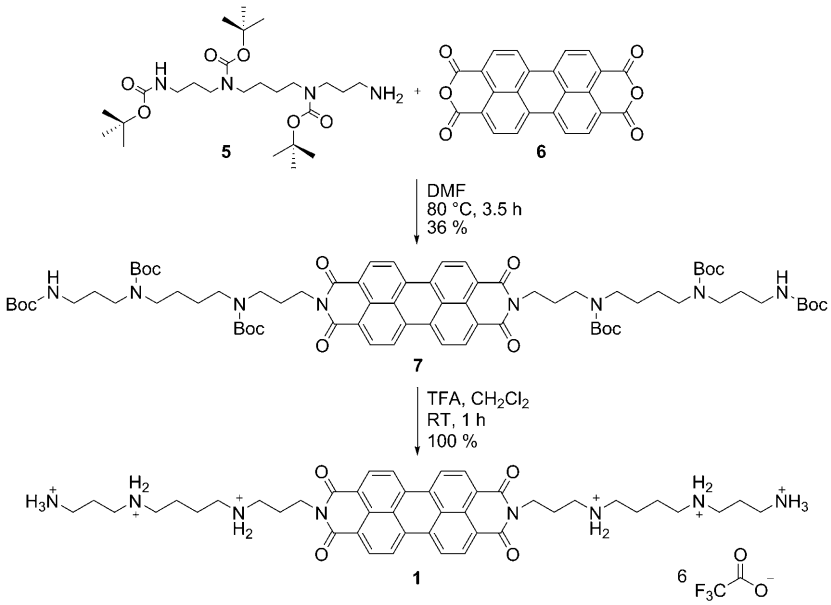

Scheme 1. Synthesis of PBI **1**.

Polyamines represent another class of highly hydrophilic compounds that can be used as excellent solubility-enhancing residues for investigations in water.[22] They also offer biological activity in many respects and play a major role in a huge variety of genetic processes, such as DNA replication, gene expression, and gene delivery.[23] In our initial study, we introduced the biologically active polyamine spermine into the bay region of the perylene core.[24] We showed that the protonated polyamines act as solubilizing moieties in aqueous solutions as well as a fluorescent probe that interacts with the negatively charged sugar phosphate backbone of calf thymus DNA. At the same time, the groups of Savino and Franceschin reported on PBIs bearing several amines and polyamines in the imide position of the perylene bisimide dye. This mode of substitution sustains the planar structure of the perylene core, which makes the system very interesting for intercalation experiments, in particular with guanine-rich DNA.[25]

Owing to their planarity, the formation of self-assembled nanostructures is also possible for core-unsubstituted PBIs by the pronounced π–π-stacking interactions of these chromophores in water.[18] Here we present the synthesis of a series of four highly water-soluble amphiphilic PBIs **1–4** that incorporate spermine residues at the imide positions. Different spectroscopic studies in aqueous solution (UV/Vis and fluorescence spectroscopy) and on the solid surface [atomic force microscopy (AFM) and transmission electron microscopy (TEM)] disclosed the aggregation behavior of these bola-amphiphilic systems[26] depending on the length of their alkyl chain interconnections.

Results and Discussion

Synthesis of PBIs 1–4: The synthesis of compound **1**, in which spermine is directly connected to the perylene bisimide, was achieved in two steps (Scheme 1). Threefold *tert*-butoxycarbonyl-protected (Boc-protected) spermine **5** was synthesized according to literature procedures[27] and directly reacted with perylenetetracarboxylic bisanhydride (**6**) in DMF at 80 °C to give the fully protected precursor **7** in 36 % yield. The protecting groups were removed by the addition of trifluoroacetic acid to a solution of **7** in dichloro-

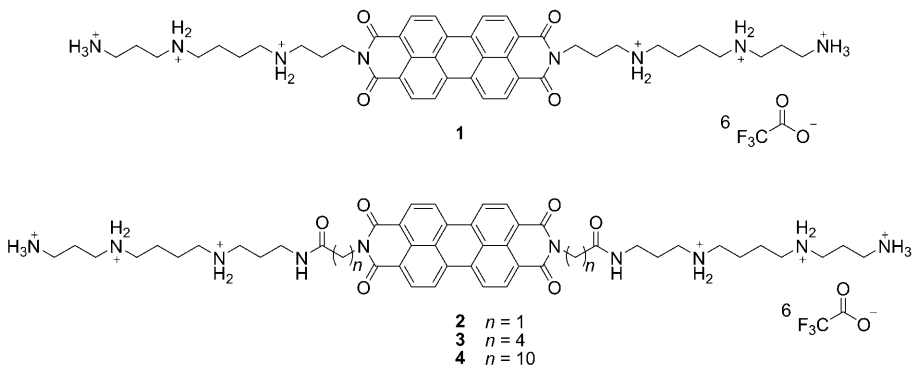

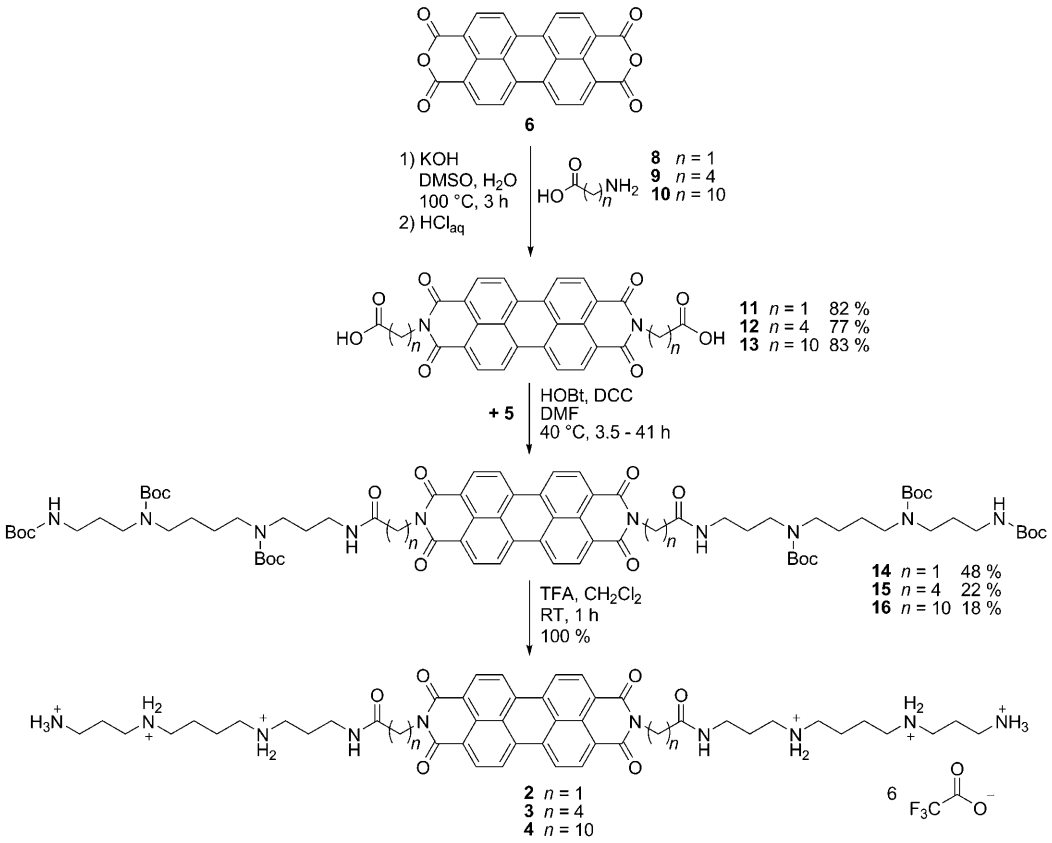

Scheme 2. Synthesis of PBIs **2**, **3**, and **4** with alkylcarbonyl interconnectors of different lengths.

methane. The trifluoroacetate salt **1** was obtained as a dark red solid after removal of the solvent and lyophilization from water. PBI **1** was characterized by ^{1}H NMR, HRMS, UV/Vis, and fluorescence spectroscopy.

Compounds **2**, **3**, and **4** were synthesized in three steps according to the route depicted in Scheme 2. The respective dicarboxylates **11**–**13** were obtained according to literature procedures with some modifications in the workup.[28] A solution of the corresponding ω-aminocarboxylic acid [glycine (**8**), $n=1$; 5-aminovaleric acid (**9**), $n=4$; 11-aminoundecanoic acid (**10**), $n=10$] with potassium hydroxide in water was added to a hot suspension of **6** in DMSO. The mixture was vigorously stirred at 100 °C for 3 h. The reaction solution was then cooled to room temperature. After adjustment of the solution to pH 5 by the use of aqueous hydrochloric acid, the resulting precipitate was collected by centrifugation. After several washing steps with water and methanol, the red solid was treated with hot aqueous hydrochloric acid (2 M) and filtered. Compounds **11**, **12**, and **13** were obtained in 82, 77, and 83 % yield, respectively, on the basis of starting compound **6**. Due to their low solubility, compounds **11**, **12**, and **13** were characterized only by FTIR spectroscopy, their melting points, and HRMS.

In the second step, the corresponding dicarboxylic acids were activated by *N*,*N*-dicyclohexylcarbodiimide (DCC) and 1-hydroxybenzotriazole (HOBt) in DMF. After addition of threefold Boc-protected spermine **5**, the reaction solutions were stirred for up to 41 h at 40 °C. After dilution with water and subsequent extraction with CH_2Cl_2, the crude product was purified by standard column chromatography followed by HPLC. The Boc-protected precursors **14**, **15**, and **16** could be isolated in yields of 48, 22, and 18 %, respectively, and were characterized by ^{1}H NMR and UV/Vis spectroscopy and HRMS. Removal of the protecting groups led to the trifluoroacetate salts **2**, **3**, and **4**, respectively, in quantitative yield. These compounds were lyophilized from water and characterized by ^{1}H NMR, UV/Vis, and fluorescence spectroscopy and HRMS.

Aggregation studies by UV/Vis spectroscopy: Because of their good solubility even in pure water, we could investigate the UV/Vis absorption properties of the trifluoroacetate salts of twofold spermine-functionalized perylene bisimide dyes **1**–**4** in this solvent over a wide concentration range. Figure 1 A shows the absorption spectra of **1** in the concentration range 4×10^{-3} to 7×10^{-7} M. All spectra display an absorption band between 400 and 625 nm related to the S_0–S_1 electronic transition of the PBI chromophore. At low concentrations, the well-resolved vibronic structure with the 0–0, 0–1, and 0–2 transitions can be recognized with the two most intense bands at 533 nm ($\varepsilon=70\,100\,M^{-1}cm^{-1}$) and 497 nm ($\varepsilon=45\,500\,M^{-1}cm^{-1}$). Pronounced spectral changes could be observed with increasing concentration of PBI **1**. Concomitantly, the color of the solution changed from

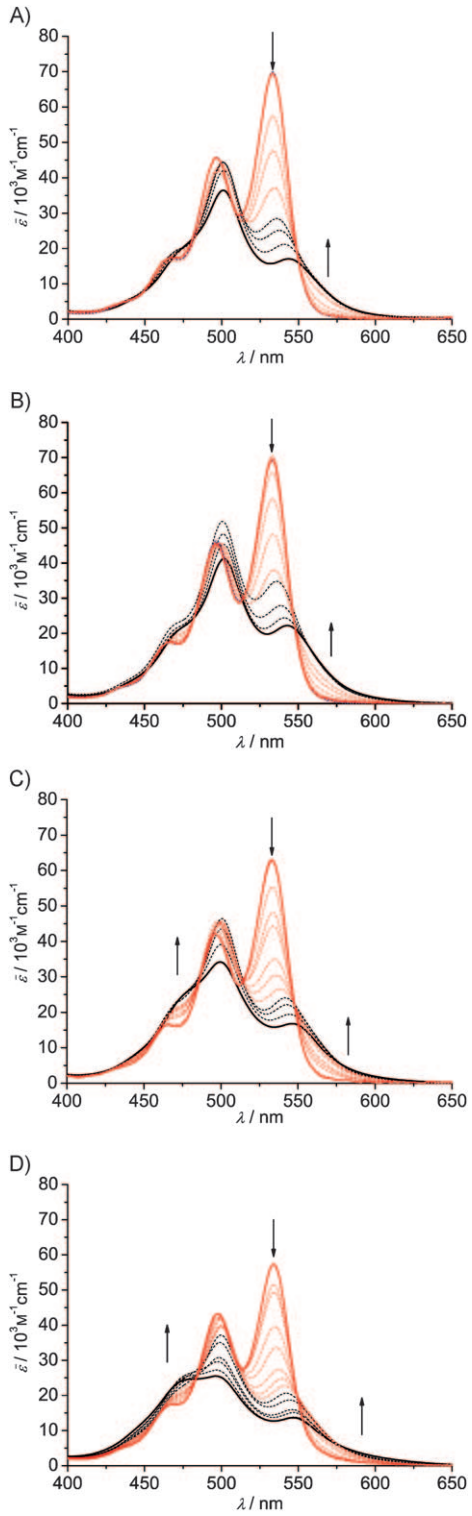

Figure 1. Absorption spectra of PBIs **1**–**4** in water: A) **1**, $c=4\times10^{-3}$ to 7×10^{-7} M; B) **2**, $c=5\times10^{-3}$ to 1×10^{-6} M; C) **3**, $c=5\times10^{-3}$ to 5×10^{-7} M; D) **4**, $c=5\times10^{-3}$ to 5×10^{-7} M. The red curves represent the low concentration range: A) **1**, $c_{low}=2\times10^{-4}$ to 7×10^{-7} M; B) **2**, $c_{low}=3.5\times10^{-4}$ to 5×10^{-7} M; C) **3**, $c_{low}=2\times10^{-4}$ to 5×10^{-7} M; D) **4**, $c_{low}=1\times10^{-4}$ to 5×10^{-7} M.

bright orange (owing to luminescence) in diluted samples to a deep red for the concentrated ones. The absorption maximum was shifted from 533 to 501 nm with a significant decrease of the absorption coefficient ($\varepsilon=36400\,M^{-1}cm^{-1}$). Furthermore, the absorption increased in the range between 550 and 600 nm. Both phenomena indicate aggregation of the PBI dyes in an H-type manner with rotational displacement, similar to what has been observed for other core-unsubstituted PBI dyes in aliphatic solvents.[29]

If the absorption spectra of, for example, **1** are considered in only the low concentration range between 2×10^{-4} and 7×10^{-7} M (red curves, Figure 1A), isosbestic points at 549 and 514 nm are evident. These crossover points indicate the existence of two species in equilibrium. At highest dilution ($c<10^{-6}$ M) the two most intense bands have a ratio of 0.65, which points to the predominant existence of PBI **1** in its monomeric form.[30] Thus, the equilibrium most likely represents the transition from monomeric PBI **1** to its dimeric form. A dimerization constant of approximate $10^4\,M^{-1}$ could be estimated.[31] At higher concentrations ($c>2\times10^{-4}$ M) the growth toward extended oligomers of **1** seems to take place, because the spectra at this concentration range no longer cross through the isosbestic points and are broadened (black curves, Figure 1A).

For PBI **2** with a methylenecarbonyl linker between the PBI and the spermine subunit, we found similar absorption behavior (Figure 1B). In the concentration range from 5×10^{-3} to 5×10^{-7} M the absorption changed from a typical monomer spectrum of PBIs with the two most intense bands at 533 and 497 nm ($\varepsilon=70000$ and $45300\,M^{-1}cm^{-1}$, respectively, ratio 0.65) to a broader spectrum with a less resolved vibronic pattern. The absorption maximum shifted hypsochromically to 502 nm and the absorption coefficient dropped to $41200\,M^{-1}cm^{-1}$. The monomeric form appears to be favored more in PBI **2** than it does in PBI **1**, because the decrease of the absorption coefficient is less pronounced for PBI **2** in the same concentration range. As in the case of compound **1**, isosbestic points occur in the lower concentration range of the absorption spectra (3.5×10^{-4} to 5×10^{-7} M) of PBI **2** at 546 and 514 nm. For more concentrated solutions, the spectra also indicate the formation of larger oligomers, as they do not fit to the isosbestic points anymore and appear broadened. Likewise, PBI **3**, possessing a butylcarbonyl linker, exhibits very similar absorption behavior on increasing concentration (Figure 1C).

In contrast to PBI dyes **1**–**3**, chromophore **4** does not show the (typical) bright orange color of bay-unsubstituted PBIs in low concentrated aqueous solution. Already for the least concentrated solution (5×10^{-7} M), aggregated species seem to be present, as indicated by the ratio of the two bands at 498 nm ($\varepsilon=43200\,M^{-1}cm^{-1}$) and 534 nm ($\varepsilon=57300\,M^{-1}cm^{-1}$) of 0.75 (Figure 1D); this is considerably higher than the ratios observed for PBIs **1**–**3** at lowest concentration. Upon increasing the concentration a rather high absorption in the bathochromic region of 550–600 nm and the formation of a distinct shoulder at about 475 nm appear; this indicates strong aggregation of PBI **4** leading to a unique aggregate structure.

The absorption spectra of PBIs **1**–**4** indicate that the degree of aggregation is dependent on the existence and the length of the alkylcarbonyl spacers linking the perylene bisimide with the spermine moieties. PBI **2**, which has only one CH_2 group between the building blocks, shows least aggregation in this series. Although the aggregation behavior of **2** is very similar to that of PBI **1**, the latter possesses a higher aggregation propensity, even though the spermine moiety is directly connected to the perylene bisimide. Apparently, the polar effect of the amide bond in **2** prevails over the CH_2 group and hence leads to the most polar environment around the chromophore core within this series. For compound **3**, with four CH_2 groups, aggregation is more pronounced and initiates already at lower concentration compared to that of **1** and **2**. The ten CH_2 groups of PBI **4** have the strongest influence on the aggregation. The π–π-stacking of the chromophore in combination with the van der Waals interactions between the alkyl chains lead already at the lowest concentration to distinct aggregates of **4** in water.

It is worth noting that the pH values of aqueous solutions of PBIs **1**–**4** were not constant over the concentration range applied here. The pH values varied between 4 for the most concentrated solutions to 7 for the most dilute ones. Evidently, this effect originates from the acidic character of the ammonium functional groups of the imide substituents. Presumably, upon aggregation of the monomers the positive charges of the spermine residues come in close contact to each other and form a cationic microenvironment around the chromophore. To prevent this destabilizing interaction between equally charged groups, protons are released to the bulk solvent leading to a decrease of the pH. On the other hand, the existence of free amine groups facilitates the formation of hydrogen bonds between charged ammonium and neutral amine groups, resulting in a stabilized aggregate. However, with increasing length of the aggregate, the donation of protons results in a critical pH value, which prohibits a further release of protons into the bulk solvent.[32]

This equilibrium between deprotonation and reprotonation of the spermine moieties can be regarded as a self-regulating system and might be the reason why PBIs **1**–**4** do not act as hydrogelators. Hence, pure aqueous solutions of PBIs **1**–**4** are stable against precipitation over months. In contrast,

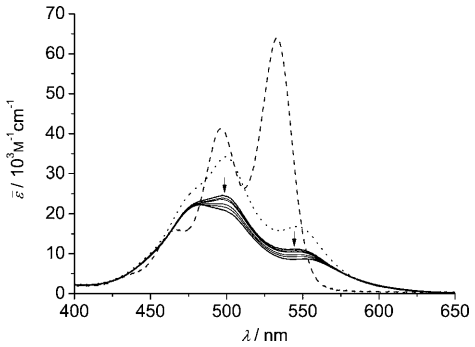

Figure 2. UV/Vis spectra of PBI **3** in phosphate buffer (10 mM, pH 7, 25 °C) in the concentration range 5×10^{-4} to 5×10^{-6} M (black lines; arrows indicate the spectral changes upon increasing concentration); PBI **3** in pure water at $c=5\times10^{-4}$ M (dotted line) and 5×10^{-6} M (dashed line).

attempts to measure the concentration-dependent aggregation behavior of PBIs **1**–**4** in phosphate buffer solution (10 mM, pH 7, ionic strength 148 mM, 25 °C) were hampered by partial precipitation of the aggregates. According to literature reports, spermine is fully protonated at a physiological pH of 7.4,[33] and thus prevents the precipitation of the dyes. In basic solutions (pH ≥ 8) the spermine residues are deprotonated, resulting in the precipitation of the dyes due to a reduced solubility in water. Figure 2 shows the spectra of PBI **3** in phosphate buffer within a concentration range of 5×10^{-4} M to 5×10^{-6} M (black lines). Already for the most dilute concentration (5×10^{-6} M), the absorption maximum is observed at a lower wavelength of 497 nm ($\varepsilon=24\,600\,M^{-1}cm^{-1}$); this points to the presence of extended aggregates. When the concentration is increased, there is a further hypsochromic shift of the absorption maximum to 483 nm ($\varepsilon=22\,300\,M^{-1}cm^{-1}$). The second absorption band appears at 547 nm ($\varepsilon=11\,100\,M^{-1}cm^{-1}$) and shifts bathochromically to 552 nm ($\varepsilon=8700\,M^{-1}cm^{-1}$) in the most concentrated sample.

The position of these absorption maxima and the rather low absorption coefficients compared to those of PBI **3** in pure water (Figure 2; dashed and dotted lines) are indicative for the formation of even larger aggregates. Two reasons might be responsible for this extended aggregation: first, the buffer absorbs the released protons upon increasing concentration and thus impedes the decrease of the pH of the solutions (contrary to the behavior in pure water) and, second, the higher ionic strength of the solution might suppress the electrostatic self-repulsion within the cationic residues and favor stacking interactions.[34]

Fluorescence spectroscopy: Fluorescence emission spectra of PBIs **1**–**4**, measured in water solutions, are shown in Figure 3, together with the corresponding UV/Vis absorption spectra. The emission spectra of **1**, **2**, and **3** in dilute solutions, which are supposed to contain predominantly monomeric dyes, are mirror images of the corresponding absorption spectra with Stokes shifts of around 13 nm. The fluorescence quantum yields range from 0.90 for **1** to 0.78 for **2** and 0.72 for **3**, and are noticeably high for perylene bisimide dyes in aqueous solution. The fluorescence emission spectrum of PBI **4** (Figure 3D) was recorded at a concentration (5×10^{-7} M) at which the dye molecules did not predominantly exist as monomers according to the absorption spectrum. Nevertheless, the fluorescence emission spectrum of **4** displays the typical shape of monomeric PBIs, whilst the fluorescence quantum yield is with 0.39, notably lower than those for PBIs **1**–**3**.

The obtained fluorescence quantum yields are not easy to interpret due to the concentration-dependent aggregation of the spermine-functionalized PBIs and the possibility of the formation of excited-state PBI aggregates (excimers).[35] Except for PBI **4**, all emission spectra represent the mirror image of the respective monomer absorption spectra and thus corroborate the existence of monomeric PBIs in the excited state within the appropriate concentration range. Like-

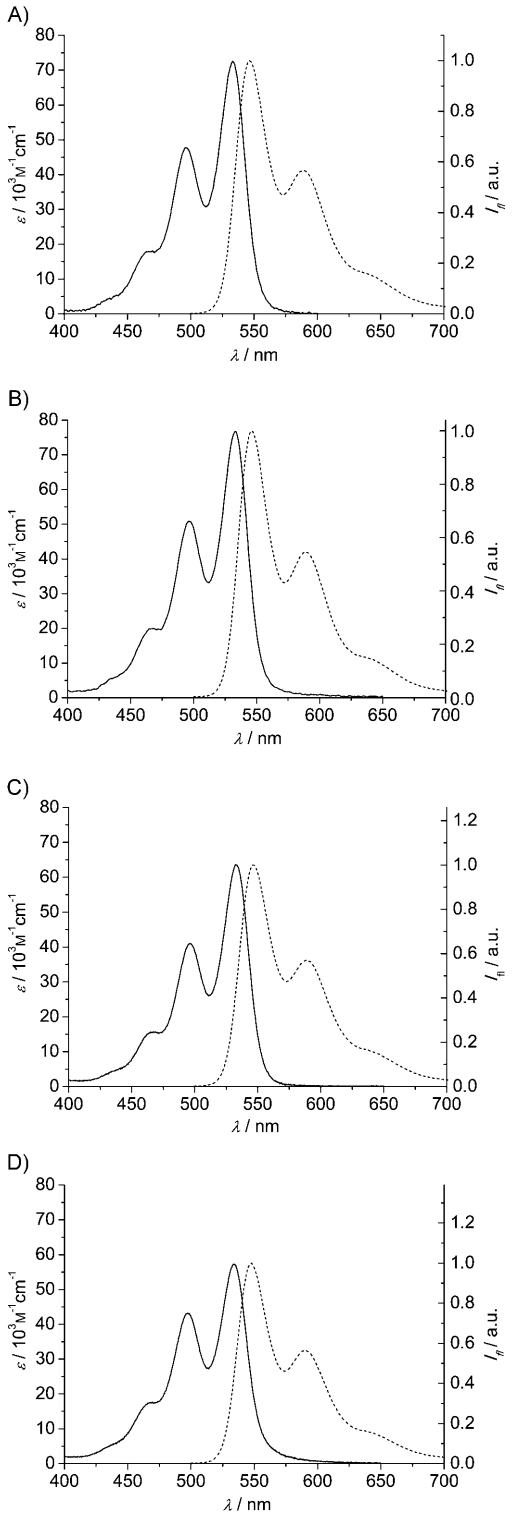

Figure 3. Absorption (solid lines) and emission (dotted lines) spectra of PBI **1**–**4** in water: A) **1**, $c=7\times10^{-7}$ M, $\Phi_{fl}=0.90$; B) **2**, $c=5\times10^{-7}$ M, $\Phi_{fl}=0.78$; C) **3**, $c=5\times10^{-7}$ M, $\Phi_{fl}=0.72$; D) **4**, $c=5\times10^{-7}$ M, $\Phi_{fl}=0.39$; excitation wavelength 475 nm; internal standard 0.1 N NaOH solution of fluorescein.

wise, a single exponential fluorescence decay and a fluorescence lifetime of 4.0 ns was recorded for a 5×10^{-7} M solution of PBI **2** in water (see Figure S3 in the Supporting Information), which is in agreement with the literature data found for monomers of bay-unsubstituted perylene bisimides.[29c] However, with increasing spacer length, and thus higher propensity for aggregation, the fluorescence quantum yield is reduced from 0.90 (**1**) to 0.39 (**4**). As the shape of the emission spectrum of **4** is identical to those of **1**, **2**, and **3**, it may be concluded that only (or rather predominantly) the excited monomers that are present in equilibrium contribute to emission; in the case of PBI **4**, this is around 40%.

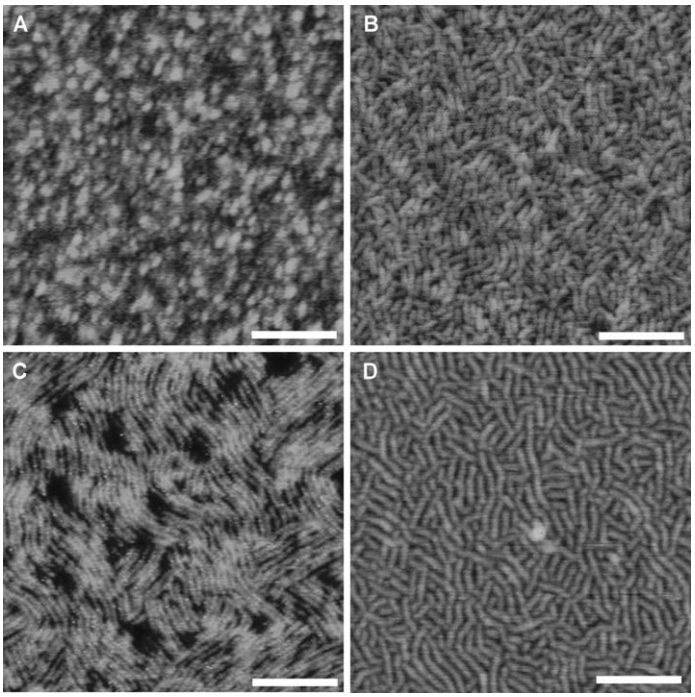

Figure 4. AFM tapping mode images (height) of films prepared from fresh aqueous solutions of **1** (A), **2** (B), **3** (C), and **4** (D) spin-coated onto mica ($c=1\times10^{-3}$ M). The scale bar corresponds to 50 nm and the z scale is 1 nm.

Two important conclusions can be drawn from these studies: first, simple PBI dyes without any substituents in the bay area can become excellent fluorophores even in water, if their aggregation is prohibited, and, second, polycationic side chains in the imide positions are particularly suited to inhibit aggregation, because their repulsive forces sustain the excited state of the dyes.

Atomic force microscopy (AFM) and transmission electron microscopy (TEM) experiments: To obtain better insights into the aggregate structure of PBIs **1**–**4**, tapping-mode AFM images were recorded at a concentration of 1×10^{-3} M in water. The samples were spin-coated from freshly prepared water solutions on mica and after aging of the solution for one month to investigate the time-dependent growth of supramolecular structures.

Figure 4 depicts the topography images of thin films spin-coated from freshly prepared solutions of PBIs **1**–**4** onto mica. The height image of compound **1** shows small globular structures with a mean diameter of 3–6 nm (Figure 4 A).

Over one month, the shape and size of the structures did not change (see Figure S1 A in the Supporting Information). Compared to this result, PBI **2** reveals a completely different morphology on the mica surface. Rod-like structures with a mean diameter of 3.9 ± 0.3 nm and lengths of up to 40 nm cover the whole surface, hence circumventing a height measurement (Figure 4 B). The aged solution of **2** shows even longer structures, indicating a slow growth process of the nanorods in solution (see Figure S1 B in the Supporting Information). Figure 4 C displays the results for the freshly prepared solution of compound **3**. Long, straight rods of about 4.8 nm in diameter form lamellae-like networks both for the freshly prepared solution and for the aged sample (see Figure S1 C in the Supporting Information). In this case, a cross-section analysis was possible, and a mean height of 1.3 nm could be determined (see Figure S2 in the Supporting Information). The rather low value might result from both the strong ionic interaction of the positively charged spermines with the predominantly negative charged mica surface, as well as from the deformation of such a soft surface by the tip during the measurement in tapping mode.[36] The rods of PBI **3** align more parallel than those of compound **2**, and show a woven network. For compound **4**, the images of the fresh and aged samples cannot be distinguished (Figure 4 D and Figure S1 D in the Supporting Information). Very long, worm-like structures 5.5 ± 0.5 nm in diameter cover the whole surface. The lengths of the rods cannot be determined with high accuracy, due to the interwoven pattern on the surface. However, a rough estimation reveals lengths of up to 200 nm.

Although a precise size analysis of the rod aggregates is not possible due to close packing on the surface, some conclusions can be reasonably drawn on the basis of the AFM observations. With increasing length of the imide substituents, the growth of nanorods is favored, both in diameter (minimum 3.6 nm for PBI **2** and maximum 6.0 nm for PBI **4**) and in length (minimum 20 nm for PBI **2** and $\approx$200 nm for PBI **4**). This diameter can be related to the dimension of the longitudinal axis of the monomers, whereas the length of the worm-like objects depends on the number of monomers forming the aggregates by π–π-stacking interactions. As the increase in diameter is caused by an increase of the spacer length, aggregation is promoted by the more hydrophobic character of the molecules in aqueous solution. Moreover, the time-dependent growth within one month is also influenced by the length of the imide substituents, because aggregates of PBI **1** do not grow at all within one month, whereas the length of PBI **2** aggregates nearly doubled.

Furthermore, we have investigated the aggregation behavior of PBI **4** by TEM. Figure 5 A shows the TEM image of a film from a freshly prepared solution of **4** in water, drop-cast on the carbon-coated copper grid and stained with uranyl acetate solution. There are numerous short rods and only few are of extended lengths. The diameter of these rods is about 6–9 nm. This is slightly bigger than the diameter obtained from AFM data (5.5 ± 0.5 nm). The increased

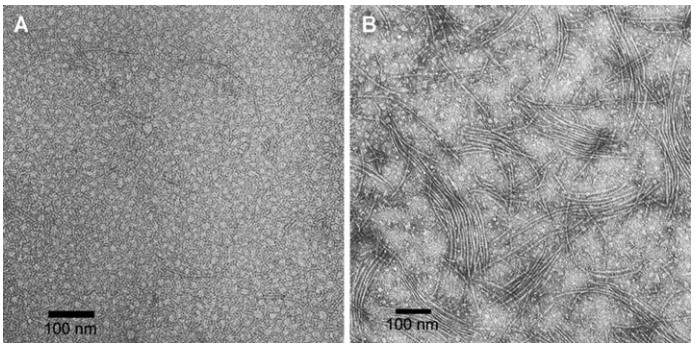

Figure 5. TEM images of films prepared from a solution of **4** in water ($c = 1 \times 10^{-3}$ M) cast on a carbon-coated copper grid: A) from a freshly prepared solution; B) from a solution aged for one month.

value most likely results from the swollen hydrophilic shell of the bola-amphiphile upon staining. The white interior represents the less polar and thus almost unstained perylene core and the black outer area occurs due to the well-stained ionic spermine substituents. This contrast pattern underlines again the amphiphilic character of the PBIs presented here. After aging of the solution for one month (Figure 5 B), the long rods can be recognized more precisely, and they are the dominant species on the carbon-coated copper grid. The length of the rods had increased, whereas the diameter remained unchanged, suggesting that no morphology change took place.

Molecular modeling: Towards a structure model for the self-aggregated PBIs **1**–**4**, force-field calculations were performed (for details, see Supporting Information). Molecular dynamics studies were used to simulate the stacking of six molecules of PBI **1** and PBI **4**, respectively, in a time slot of 500 ps at 300 K (snapshots of the appropriate arrangement were taken every 50 ps). Figure 6 A shows the superimposed structures of six stacked molecules of PBI **1**. The top view reveals clearly the separation of the rather stiff and unpolar perylene core and the far more flexible shell of hydrophilic spermine residues. The oxygen atoms of the bisimide groups

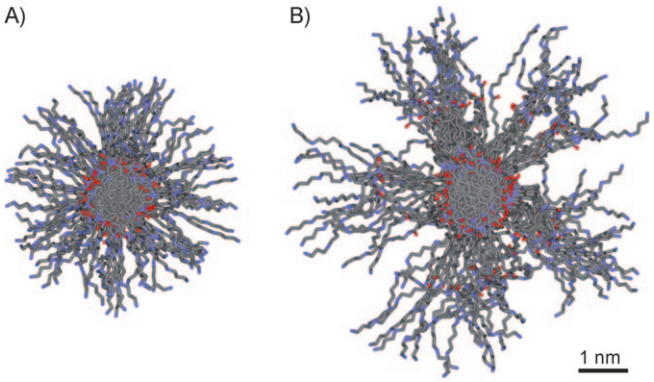

Figure 6. Top view of ten superimposed structures of six stacked molecules (60 molecules in total) of PBI **1** (A) and PBI **4** (B) (gray = carbon, red = oxygen, blue = amine; hydrogen atoms are omitted for clarity).

mark the border between the hydrophilic outer shell based on spermine residues and the inner cylinder of hydrophobic perylene cores. The overall diameter is approximately 4.3 nm, whereas the interior hydrophobic core has a diameter of about 1.5 nm. Figure 6B presents the overlay of six molecules of PBI **4** under the same conditions as for PBI **1**. Again, the π–π-stacked inner core is the central element. Compared to the shell of the PBI **1** stack, the introduction of the alkylcarbonyl linkers led to an apportionment of the shell (overall diameter ca. 6.2 nm). Hydrophobic interactions force the alkyl chains to a surface less accessible to solvent, underlining the stronger overall interaction between the bola-amphiphiles. At the outer rim of the PBI **4** stack the spermine residues behave in the same manner as in the case of PBI **1**, because the protonated polyamines form brush-like structures under intensive interaction with the polar solvent. Hence the calculations corroborate the importance of the alkyl linkers for the enhanced aggregation of PBI **4**.

Conclusions

In summary, we have synthesized four twofold spermine-functionalized and core-unsubstituted perylene bisimides. Three of them incorporate alkylcarbonyl linkers of different lengths between the chromophore and the polyamine spermine (PBI **2**–**4**), whereas in PBI **1** a terminal amino group of spermine provides the imide nitrogen of the perylene bisimide dye. These PBI derivatives are highly water soluble owing to protonation of the amine groups of the spermine residues. At high dilution, the PBIs presented here exhibit a very high fluorescence quantum yield (Φ_{fl}) of up to 0.90 for PBI **1** in water. With increasing linker length, the Φ_{fl} value decreases to 0.39 for PBI **4**. Both UV/Vis and fluorescence spectra confirm the formation of H-type aggregates at higher concentration by efficient stacking of the planar π-system of the chromophores. AFM and TEM studies reveal the formation of large rod-like aggregates that grow both in length and diameter with increasing linker length. Finally, force-field calculations illustrate the dynamic behavior of the PBI-based bola-amphiphiles with a rather stiff inner core and a flexible outer shell. Our results demonstrate that perylene bisimides can be outstanding fluorophores in aqueous media as well, if their aggregation is efficiently suppressed. This observation might open a new research avenue for this popular class of functional dyes.

Experimental Section

General: Solvent and reagents were purchased from commercial sources, unless otherwise stated, and purified and dried according to standard procedures.[37] Reactions were monitored by TLC on silica gel plates (Merck TLC silica gel 60 F_{254} aluminum sheets). All perylene derivatives are colored, so no additional visualization of the spots was necessary. Amines were visualized by spraying the TLC plate with ninhydrin solution.[38] Column chromatography was performed on silica gel (Merck Silica 60, particle size 0.04–0.063 mm). Semipreparative HPLC was performed on a Jasco system (PU 2080 PLUS) with a UV/Vis detector (UV 2077 PLUS) and using a semipreparative NUCLEOSIL C8 column (Macherey & Nagel). NMR experiments were conducted on a Bruker Avance 400 spectrometer with TMS or residual undeuterated solvent as internal standard. The chemical shifts are reported in ppm relative to TMS (δ scale). The apparent coupling constants J are given in Hertz (Hz). The following abbreviations are used to describe the signal fine structure: s = singlet, brs = broad singlet, d = doublet, t = triplet, q = quartet, dt = doublet of triplets, tt = triplet of triplets, and m = multiplet. All IR spectra[39] were measured of samples prepared as KBr pellets on a Jasco FTIR 410 spectrophotometer. The IR data are reported in the Supporting Information. All melting points were measured on a Linkam TP 94 heating stage and are uncorrected. Mass spectra were performed on Bruker MALDI-TOF (autoflex II) and Bruker ESI-TOF (microTOF focus) spectrometers.

UV/Vis spectroscopy: All absorption spectra were measured on a Perkin–Elmer Lambda 950 spectrometer equipped with a Peltier system as temperature controller; samples were placed in conventional quartz cells of appropriate path length. The spectral bandwidth and the scan rate were 2 nm and 140 nm min^{-1}, respectively. Either spectroscopically pure dichloromethane (Uvasol) or MilliQ water was used for measurements. The stock solutions for the concentration-dependent measurements of PBIs **1**–**4** were prepared by accurately weighing the Boc-protected precursors. After deprotection, the fluffy red solids were dissolved in an appropriate amount of MilliQ water to give the stock solution. Dilutions of these stock solutions were used for absorption measurements over the indicated concentration range.

Fluorescence spectroscopy: All emission spectra were recorded on a PTI QM4–2003 fluorescence spectrometer and were corrected against photomultiplier and lamp intensity. A long wavelength range emission corrected Hamamatsu photomultiplier R928 was used. Quartz glass cuvettes with a thickness of 10 mm were used for the measurements. Fluorescence quantum yields Φ_{fl} were determined in MilliQ water vs. fluorescein (Φ_{fl} = 0.92 in 0.1 N NaOH) as reference.[40] The given quantum yields are averaged from values measured at three different excitation wavelengths with OD 0.02–0.05 in the absorption maximum (standard deviation σ = 1–3 %).

AFM: All investigations were performed under ambient conditions using a Veeco MultiMode Nanoscope IV system operating in tapping mode in air. Silicon cantilevers (Olympus Corporation, Japan) with a resonance frequency of ≈300 kHz were used. Samples of **1**–**4** were prepared by spin-coating either a fresh or an aged solution (stored one month at room temperature in a sealed tube) in MilliQ water onto freshly cleaved mica at 7000 rpm.

TEM: TEM measurements were performed on a Siemens Elmiskop 101 Electron Microscope, operating at an acceleration voltage of 80 kV. For the observation of aggregates, a drop of sample suspension (PBI **4**, $c = 1 \times 10^{-3}$ M in water) was placed on 400-mesh formvar copper grids coated with carbon. About 2 min after the deposition, the grid was tapped with filter paper to remove surface water. Negative staining was performed by the addition of a drop of an aqueous solution of uranyl acetate (0.5 %) onto the copper grid. After 1 min, the surface water on the grid was removed by taping with filter paper.

Synthesis and characterization of PBIs

PBI 7: Perylenetetracarboxylic acid bisanhydride (**6**; 138 mg, 3.52 μmol) and threefold Boc-protected spermine **5**[27] (390 mg, 7.76 μmol) were suspended in dry DMF (3 mL) and stirred for 3.5 h at 80 °C. The reaction solution was transferred into a separatory funnel and diluted with water (10 mL) and CH_2Cl_2 (70 mL). The organic phase was washed with water (3 × 40 mL). After phase separation, the aqueous phase was extracted with CH_2Cl_2 (2 × 15 mL). The organic phases were combined and dried over magnesium sulfate. The solvent was removed in vacuo and the residual crude product was purified by column chromatography (silica gel, CH_2Cl_2/MeOH 97:3) and HPLC (Nucleosil, CH_2Cl_2/MeOH 98:2); this gave the fully protected precursor **7** as a red solid in 36 % yield (170 mg, 125 μmol). MW ($C_{74}H_{104}N_8O_{16}$) = 1361.66 g mol^{-1}; R_f = 0.31 (CH_2Cl_2/MeOH 98:2); m.p. 128 °C; ^{1}H NMR ($CDCl_3$): δ = 8.69 (d, J = 7.96 Hz,

4H), 8.62 (d, $J=8.08$ Hz, 4H), 4.23 (dt, $J_{CHCH}=7.14$ Hz, 4H), 3.33, 3.25, 3.15, 3.09 (brs, 20H), 2.01 (tt, $J=7.68$, 6.96 Hz, 4H), 1.66 (brs, 4H), 1.52 (brs, 8H), 1.45, 1.43 ppm (s, 18H+36H); the carbamate NH signal is not detectable due to the fast exchange with the deuterated solvent; UV/Vis (CH_2Cl_2): λ_{max} (ε_{max}) = 525 nm (80500 $M^{-1}cm^{-1}$); MS (MALDI, matrix: DCTB): calcd for $C_{74}H_{104}N_8O_{16}+e^-$: 1360.757 $[M]^-$; found: 1360.755; HRMS (ESI+): *m/z*: calcd for $C_{74}H_{104}N_8O_{16}+Na^+$: 1383.7467; found: 1383.7467.

General procedure for the synthesis of fully protected precursors 14–16: A mixture of the appropriate dicarboxylic acid (0.20 mmol, 1 equiv), threefold Boc-protected spermine **5** (2.2 equiv), DCC (3 equiv), and HOBt (0.5 equiv) in DMF (3 mL) was stirred at 40 °C for 20 h under inert gas. The reaction solution was diluted with water and extracted with CH_2Cl_2 (3×50 mL). The organic phases were dried over magnesium sulfate and concentrated under vacuum. The residue was purified by column chromatography and HPLC.

PBI 14: Column chromatography: silica gel, CH_2Cl_2/MeOH 98:2; HPLC: Nucleosil, CH_2Cl_2/MeOH 97:3; yield: 141 mg (0.1 mmol, 48%) of a red solid; MW ($C_{78}H_{110}N_{10}O_{18}$) = 1475.76 g mol^{-1}; $R_f=0.27$ (CH_2Cl_2/MeOH 98:2); m.p. 289 °C (decomp); ^1H NMR ([D$_6$]DMSO): $\delta=8.86$ (d, $J=7.16$, 4H), 8.62 (d, $J=7.88$, 4H), 8.17 (brs, 2H), 6.72 (brs, 2H), 4.64 (s, 4H), 3.10 (brs, 20H), 2.87 (dt, $J_{CHCH}=6.44$ Hz, $J_{NHCH}=6.24$ Hz, 4H), 1.60 and 1.55 (brs , 8H), 1.36 (s, 18H), 1.35 (s, 36H), 1.28 ppm (s, 16H); the amide and carbamate NH signals are broadened due to the fast exchange with the deuterated solvent; UV/Vis (CH_2Cl_2): λ_{max} (ε_{max}) = 525 nm (84100 $M^{-1}cm^{-1}$); HRMS (ESI+): *m/z*: calcd for $C_{78}H_{110}N_{10}O_{18}+Na^+$: 1497.7892; found: 1497.7924.

PBI 15: Column chromatography: silica gel, CH_2Cl_2/MeOH 98:2 to 97:3; HPLC: Nucleosil, CH_2Cl_2/MeOH 97:3; yield: 68.5 mg (0.044 mmol, 22%) of a red solid; MW ($C_{84}H_{122}N_{10}O_{18}$) = 1559.92 g mol^{-1}; $R_f=0.31$ (CH_2Cl_2/MeOH 98:2); m.p. 120–121 °C; ^1H NMR ($CDCl_3$): $\delta=8.62$ (d, $J=7.96$ Hz, 4H), 8.54 (d, $J=8.12$ Hz, 4H), 4.23 (dt, $J_{CHCH}=6.44$ Hz, 4H), 3.22, 3.14, 3.10 and 3.09 (m, 24H), 2.30 (dt, $J_{CHCH}=7.16$ Hz, 4H), 1.81 (brs, 8H), 1.65 (brs, 8H), 1.48 (brs, 8H), 1.44 and 1.43 ppm (m, 56H); the amide and carbamate NH signals are not detectable due to the fast exchange with the deuterated solvent; UV/Vis (CH_2Cl_2): λ_{max} (ε_{max}) = 525 nm (82000 $M^{-1}cm^{-1}$); HRMS (ESI+): *m/z*: calcd for $C_{84}H_{122}N_{10}O_{18}+Na^+$: 1581.8833; found: 1581.8793.

PBI 16: Column chromatography: silica gel, CH_2Cl_2/MeOH 97:3; HPLC: (Nucleosil, CH_2Cl_2/MeOH 97:3); yield: 60.0 mg (0.036 mmol, 18%) of a red solid; MW ($C_{96}H_{146}N_{10}O_{18}$) = 1728.24 g mol^{-1}; $R_f=0.30$ (CH_2Cl_2/MeOH 98:2); m.p. 140 °C; ^1H NMR ($CDCl_3$): $\delta=8.71$ (d, $J=7.96$ Hz, 4H), 8.65 (d, $J=8.2$ Hz, 4H), 4.20 (dt, $J_{CHCH}=7.64$ Hz, 4H), 3.21, 3.13 and 3.10 (brs, 24H), 2.17 (dt, $J_{CHCH}=7.32$ Hz, 4H), 1.76 (tt, $J=5.8$, 8.56 Hz, 4H), 1.63 (brs, 12H), 1.45 and 1.43 (brs, 56H), 1.27 ppm (brs, 32H); the amide and carbamate NH signals are not detectable due to the fast exchange with the deuterated solvent; UV/Vis (CH_2Cl_2): λ_{max} (ε_{max}) = 525 nm (82800 $M^{-1}cm^{-1}$); HRMS (ESI+): *m/z*: calcd for $C_{96}H_{146}N_{10}O_{18}+Na^+$: 1750.0709; found: 1750.0602.

General procedure for the synthesis of target PBIs 1–4: The appropriate Boc-protected PBI (10 μmol) was dissolved in CH_2Cl_2 (1 mL). Trifluoroacetic acid (TFA; 1 mL) was added and the mixture was stirred at room temperature for 1 h. The solvent and trifluoroacetic acid were removed in vacuo, giving a dark red film, which was dissolved in water. The red solution obtained was lyophilized twice from water to remove traces of residual TFA. The red voluminous solid was used without further purification. Yield: 100% for each; red fluffy solid.

PBI 1: MW ($C_{56}H_{62}N_8O_{16}F_{18}$) = 1445.11 g mol^{-1}; ^1H NMR ([D$_6$]DMSO): $\delta=9.01$ (d, $J=8.24$ Hz, 4H), 8.46 (d, $J=7.84$ Hz, 4H), 8.55 (brs, 4H), 7.85 (brs, 6H), 4.17 (t, $J=6.04$ Hz, 4H), 3.06 (brs, 4H), 2.94 and 2.88 (brs, 16H), 2.05 (tt, $J=5.36$, 7.2 Hz, 4H), 1.87 (tt, $J=8.40$, 6.92 Hz, 4H), 1.61 ppm (brs, 8H); the broad signals of the ammonium group protons (8H) superimpose one signal of the perylene CH (4H); UV/Vis (H_2O, $c=7\times10^{-6}$ M): λ_{max} (ε_{max}) = 496 (46000), 533 nm (70000 $M^{-1}cm^{-1}$); fluorescence (H_2O, $\lambda_{ex}=475$ nm): $\lambda_{max}=546$ nm; $\Phi_{fl}=0.90$; HRMS (ESI+): *m/z*: calcd for $C_{44}H_{56}N_8O_4+H^+$: 761.4497; found: 761.4494.

PBI 2: MW ($C_{60}H_{68}N_{10}O_{18}F_{18}$) = 1559.21 g mol^{-1}; ^1H NMR ([D$_6$]DMSO): $\delta=8.87$ (d, $J=8.04$ Hz, 4H), 8.68 (brs, 8H), 8.51 (d, $J=7.88$ Hz, 4H), 8.44 (t, $J=5.04$ Hz, 2H), 7.94 (brs, 6H), 4.7 (s, 4H), 3.18 (dt, $J_{CHNH}=5.92$ Hz, $J_{CHCH}=5.96$ Hz, 4H), 3.00–2.86 (m, 20H), 1.89 (tt, $J=7.92$, 7.04 Hz, 4H), 1.78 (tt, $J=7.72$, 7.00 Hz, 4H), 1.65–1.62 ppm (m, 8H); the broad signals of the ammonium group protons (8H and 6H, respectively) superimpose the signals of the perylene CH (2×4H) and the amide NH (2H); UV/Vis (H_2O, $c=1\times10^{-6}$ M): λ_{max} (ε_{max}) = 496 (45300), 533 nm (70000 $M^{-1}cm^{-1}$); fluorescence (H_2O, $\lambda_{ex}=475$ nm): $\lambda_{max}=546$ nm; $\Phi_{fl}=0.78$; HRMS (ESI+): *m/z*: calcd for $C_{48}H_{62}N_{10}O_6+H^+$: 875.4927; found: 875.4911.

PBI 3: MW ($C_{66}H_{80}N_{10}O_{18}F_{18}$) = 1643.37 g mol^{-1}; ^1H NMR ([D$_6$]DMSO): $\delta=8.58$ (d, $J=8.02$ Hz, 4H), 8.30 (d, $J=7.72$ Hz, 4H), 8.03 (t, $J=5.40$ Hz, 2H), 4.03 (brs, 4H), 3.11 (dt, $J_{CHNH}=6.28$ Hz, $J_{CHCH}=6.04$ Hz, 4H), 2.98 (t, $J=7.60$ Hz, 4H), 2.92–2.86 (m, 16H), 2.18 (t, $J=7.04$ Hz, 4H), 1.89 (tt, $J=8.04$, 7.12 Hz, 4H), 1.78 (tt, $J=7.72$, 6.92 Hz, 4H), 1.63 ppm (brs, 16H); the broad signals of the ammonium group protons (8H and 6H, respectively) superimpose the signals of the perylene CH (2×4H) and the amide NH (2H); UV/Vis (H_2O, $c=5\times10^{-7}$ M): λ_{max} (ε_{max}) = 496 (42100), 533 nm (63000 $M^{-1}cm^{-1}$); fluorescence (H_2O, $\lambda_{ex}=475$ nm): $\lambda_{max}=546$ nm; $\Phi_{fl}=0.72$; HRMS (ESI+): *m/z*: calcd for $C_{54}H_{74}N_{10}O_6+H^+$: 959.5866; found: 959.5867.

PBI 4: MW ($C_{78}H_{104}N_{10}O_{18}F_{18}$) = 1811.89 g mol^{-1}; ^1H NMR ([D$_6$]DMSO): $\delta=8.68$ (brs, 8H), 8.35 (d, $J=7.54$ Hz, 4H), 8.13 (d, $J=7.4$ Hz, 4H), 7.97 (t, $J=5.44$ Hz, 2H), 3.94 (brs, 4H), 3.15 (dt, $J_{CHNH}=6.52$ Hz, $J_{CHCH}=5.96$ Hz, 4H), 2.98 (t, $J=7.48$ Hz, 4H), 2.91–2.86 (m, 16H), 2.07 (t, $J=7.20$ Hz, 4H), 1.89 (tt, $J=7.72$, 7.28 Hz, 4H), 1.71 (tt, $J=6.40$, 7.60 Hz, 4H), 1.68 (brs, 12H), 1.49 (tt, $J=7.44$, 6.92 Hz, 4H), 1.36 and 1.27 ppm (brs, 26H); the broad signals of the ammonium group protons (8H and 6H, respectively) superimpose the signals of the perylene CH (2×4H) and the amide NH (2H); UV/Vis (H_2O, $c=5\times10^{-7}$ M): λ_{max} (ε_{max}) = 497 (43200), 534 nm (57300 $M^{-1}cm^{-1}$); fluorescence (H_2O, $\lambda_{ex}=475$ nm): $\lambda_{max}=548$ nm; $\Phi_{fl}=0.39$; HRMS (ESI+): *m/z*: calcd for $C_{66}H_{98}N_{10}O_6+H^+$: 1127.7744; found: 1127.7742.

Acknowledgements

This work was supported by the Deutsche Forschungsgemeinschaft (grant: Wu 317/10).

[1] a) H. Zollinger, *Color Chemistry*, 3rd ed., Wiley-VCH, Weinheim, **2003**; b) W. Herbst, K. Hunger, *Industrial Organic Pigments: Production, Properties, Applications*, 2nd ed., Wiley-VCH, Weinheim, **1997**.

[2] a) H. Langhals, *Heterocycles* **1995**, *40*, 477–500; b) F. Würthner, *Chem. Commun.* **2004**, 1564–1579.

[3] a) F. De Schryver, T. Vosch, M. Cotlet, M. Van der Auweraer, K. Müllen, J. Hofkens, *Acc. Chem. Res.* **2005**, *38*, 514–522; b) C. Flors, I. Oesterling, T. Schnitzler, E. Fron, G. Schweitzer, M. Sliwa, A. Herrmann, M. van der Auweraer, F. De Schryver, K. Müllen, J. Hofkens, *J. Phys. Chem. C* **2007**, *111*, 4861–4870.

[4] a) D. Wöhrle, D. Meissner, *Adv. Mater.* **1991**, *3*, 129–138; b) C. Brabec, N. Sariciftci, J. Hummelen, *Adv. Funct. Mater.* **2001**, *11*, 15–26; c) L. Schmidt-Mende, A. Fechtenkötter, K. Müllen, E. Moons, R. Friend, J. MacKenzie, *Science* **2001**, *293*, 1119–1122; d) M. Sommer, M. Thelakkat, *Eur. Phys. J. Appl. Phys.* **2006**, *36*, 245–249.

[5] a) P. Ranke, I. Bleyl, J. Simmer, D. Haarer, A. Bacher, H. Schmidt, *Appl. Phys. Lett.* **1997**, *71*, 1332–1334; b) C. Ego, D. Marsitzky, S. Becker, J. Zhang, A. Grimsdale, K. Müllen, J. MacKenzie, C. Silva, R. Friend, *J. Am. Chem. Soc.* **2003**, *125*, 437–443; c) F. Jaiser, D. Neher, A. Meisel, H.-G. Nothofer, T. Miteva, A. Herrmann, K. Müllen, U. Scherf, *J. Chem. Phys.* **2008**, *129*, 114901(1–9).

[6] a) P. Malenfant, C. Dimitrakopolous, J. Gelorme, L. Kosbar, T. Graham, A. Curioni, W. Andreoni, *Appl. Phys. Lett.* **2002**, *80*, 2517–2519; b) B. Jones, M. Ahrens, M.-H. Yoon, A. Facchetti, T. Marks, M. Wasielewski, *Angew. Chem.* **2004**, *116*, 6523–6526; *Angew. Chem. Int. Ed.* **2004**, *43*, 6363–6366; c) R. Schmidt, M. Ling, J. Oh,

M. Winkler, M. Könemann, Z. Bao, F. Würthner, *Adv. Mater.* **2007**, *19*, 3692–3695.

[7] a) V. Gorteau, G. Bollot, J. Mareda, S. Matile, *Org. Biomol. Chem.* **2007**, *5*, 3000–3012; b) A. Perez-Velasco, V. Gorteau, S. Matile, *Angew. Chem.* **2008**, *120*, 935–937; *Angew. Chem. Int. Ed.* **2008**, *47*, 921–923; c) S. Hagihara, L. Gremaud, G. Bollot, J. Mareda, S. Matile, *J. Am. Chem. Soc.* **2008**, *130*, 4347–4351; d) J. Mareda, S. Matile, *Chem. Eur. J.* **2009**, *15*, 28–37.

[8] a) J. Hofkens, T. Vosch, M. Maus, F. Köhn, M. Cotlet, T. Weil, A. Herrmann, K. Müllen, F. De Schryver, *Chem. Phys. Lett.* **2001**, *333*, 255–263; b) A. Grimsdale, K. Müllen, *Angew. Chem.* **2005**, *117*, 5732–5772; *Angew. Chem. Int. Ed.* **2005**, *44*, 5592–5629; c) M. Sliwa, C. Flors, I. Oesterling, J. Hotta, K. Müllen, F. De Schryver, J. Hofkens, *J. Phys. Condens. Matter* **2007**, *19*, 445004/1–14; d) S. Melnikov, E. Yeow, H. Uji-i, M. Cotlet, K. Müllen, F. De Schryver, J. Enderlein, J. Hofkens, *J. Phys. Chem. B* **2007**, *111*, 708–719; e) K. Peneva, G. Mihov, A. Herrmann, N. Zarrabi, M. Börsch, T. Duncan, K. Müllen, *J. Am. Chem. Soc.* **2008**, *130*, 5398–5399.

[9] a) N. Rahe, C. Rinn, T. Carell, *Chem. Commun.* **2003**, 2120–2121; b) W. Wang, W. Wan, H.-H. Zhou, S. Niu, A. Li, *J. Am. Chem. Soc.* **2003**, *125*, 5248–5249; c) Y. Zheng, H. Long, G. Schatz, F. Lewis, *Chem. Commun.* **2005**, 4795–4797; d) C. Wagner, H.-A. Wagenknecht, *Org. Lett.* **2006**, *8*, 4191–4194; e) D. Baumstark, H.-A. Wagenknecht, *Angew. Chem.* **2008**, *120*, 2652–2654; *Angew. Chem. Int. Ed.* **2008**, *47*, 2612–2614; f) D. Baumstark, H.-A. Wagenknecht, *Chem. Eur. J.* **2008**, *14*, 6640–6645; g) T. Zeidan, R. Carmieli, R. Kelley, T. Wilson, F. Lewis, M. Wasielewski, *J. Am. Chem. Soc.* **2008**, *130*, 13945–13955; h) M. Hariharan, Y. Zheng, H. Long, T. Zeidan, G. Schatz, J. Vura-Weis, M. Wasielewski, X. Zuo, D. Tiede, F. Lewis, *J. Am. Chem. Soc.* **2009**, *131*, 5920–5929.

[10] J. Qu, C. Kohl, M. Pottek, K. Müllen, *Angew. Chem.* **2004**, *116*, 1554–1557; *Angew. Chem. Int. Ed.* **2004**, *43*, 1528–1531.

[11] a) X. Zhang, Z. Chen, F. Würthner, *J. Am. Chem. Soc.* **2007**, *129*, 4886–4887; b) E. Shirman, A. Ustinov, N. Ben-Shitrit, H. Weissman, M. Iron, R. Cohen, B. Rybtchinski, *J. Phys. Chem. B* **2008**, *112*, 8855–8858; c) J. Baram, E. Shirman, N. Ben-Shitrit, A. Ustinov, H. Weissman, I. Pinkas, S. Wolf, B. Rybtchinski, *J. Am. Chem. Soc.* **2008**, *130*, 14966–14967; d) G. Golubkov, H. Weissman, E. Shirman, S. Wolf, I. Pinkas, B. Rybtchinski, *Angew. Chem.* **2009**, *121*, 944–948; *Angew. Chem. Int. Ed.* **2009**, *48*, 926–930; e) E. Krieg, E. Shirman, H. Weissman, E. Shimoni, S. Wolf, I. Pinkas, B. Rybtchinski, *J. Am. Chem. Soc.* **2009**, *131*, 14365–14373; f) X. Zhang, S. Rehm, M. Safont-Sempere, F. Würthner, *Nat. Chem.* **2009**, *1*, 623–629.

[12] a) A. Ebel, W. Donaubauer, F. Hampel, A. Hirsch, *Eur. J. Org. Chem.* **2007**, 3488–3494; b) C. Schmidt, C. Böttcher, A. Hirsch, *Eur. J. Org. Chem.* **2007**, 5497–5505; c) C. Backes, C. Schmidt, F. Hauke, C. Böttcher, A. Hirsch, *J. Am. Chem. Soc.* **2009**, *131*, 2172–2184; d) C. Backes, F. Hauke, C. Schmidt, A. Hirsch, *Chem. Commun.* **2009**, 2643–2645; e) C. Ehli, C. Oelsner, D. Guldi, A. Mateo-Alonso, M. Prato, C. Schmidt, C. Backes, F. Hauke, A. Hirsch, *Nat. Chem.* **2009**, *1*, 243–249; f) C. Schmidt, C. Böttcher, A. Hirsch, *Eur. J. Org. Chem.* **2009**, 5337–5349.

[13] a) H. Langhals, W. Jona, F. Einsiedl, S. Wohnlich, *Adv. Mater.* **1998**, *10*, 1022–1024; b) Y.-M. Jeon, T.-H. Lim, J.-G. Kim, M.-S. Gong, *Macromol. Res.* **2007**, *15*, 473–477.

[14] Y. Liu, K.-R. Wang, D.-S. Guo, B.-P. Jiang, *Adv. Funct. Mater.* **2009**, *19*, 2230–2235.

[15] H.-A. Klok, H. Rodrigues, S. Becker, K. Müllen, *J. Polym. Sci. A: Polym. Chem.* **2001**, *39*, 1572–1583.

[16] T. Weil, M. Abdalla, C. Jatzke, J. Hengstler, K. Müllen, *Biomacromolecules* **2005**, *6*, 68–79.

[17] a) J. Kern, S. Kerwin, *Bioorg. Med. Chem. Lett.* **2002**, *12*, 3395–3398; b) W. Tuntiwechapikul, T. Taka, M. Béthencourt, L. Makonkewkayoon, R. Lee, *Bioorg. Med. Chem. Lett.* **2006**, *16*, 4120–4126; c) J. Zhou, G. Yuan, J. Liu, C.-G. Zhan, *Chem. Eur. J.* **2007**, *13*, 945–949; d) R. Samudrala, X. Zhang, R. Wadkins, D. Mattern, *Bioorg. Med. Chem.* **2007**, *15*, 186–193.

[18] Z. Chen, A. Lohr, C. Saha-Möller, F. Würthner, *Chem. Soc. Rev.* **2009**, *38*, 564–584.

[19] A. Margineanu, J. Hofkens, M. Cotlet, S. Habuchi, A. Stefan, J. Qu, C. Kohl, K. Mülle, J. Vercammen, Y. Engelborghs, T. Gensch, F. De Schryver, *J. Phys. Chem. B* **2004**, *108*, 12242–12251.

[20] C. Kohl, T. Weil, J. Qu, K. Müllen, *Chem. Eur. J.* **2004**, *10*, 5297–5310.

[21] K. Peneva, G. Mihov, F. Nolde, S. Rocha, J.-I. Hotta, K. Braeckmanns, J. Hofkens, H. Uji-i, A. Herrmann, K. Müllen, *Angew. Chem.* **2008**, *120*, 3420–3423; *Angew. Chem. Int. Ed.* **2008**, *47*, 3372–3375.

[22] R. Casero, P. Woster, *J. Med. Chem.* **2009**, *52*, 4551–4573.

[23] a) M. Grillo, *Int. J. Biochem.* **1985**, *17*, 943–948; b) A. Khant, Y.-H. Meit, T. Wilson, *Proc. Natl. Acad. Sci. USA* **1992**, *89*, 11426–11427; c) V. Bloomfield, *Biopolymers* **1997**, *44*, 269–282; d) J. Lewis, T. J. Thomas, A. Shirahata, T. Thomas, *Biomacromolecules* **2000**, *1*, 339–349; e) C. Wang, J. Delcros, J. Biggerstaff, O. Phanstiel, *J. Med. Chem.* **2003**, *46*, 2663–2671; f) V. Johansson, M. Miniotis, C. Hegardt, G. Jönsson, J. Staaf, P. Berntsson, S. Oredsson, K. Alm, *Cell Biol. Int.* **2008**, *32*, 1467–1477; g) A. Khomutov, T. Keinanen, N. Grigorenko, M. Hyvonen, A. Uimari, M. Pietila, M. Cerrada-Gimenez, A. Simonian, M. Khomutov, J. Vepsalainen, L. Alhonen, J. Janne, *Mol. Biol.* **2009**, *43*, 249–259.

[24] S. Krauß, M. Lysetska, F. Würthner, *Lett. Org. Chem.* **2005**, *2*, 349–353.

[25] a) L. Rossetti, M. Franceschin, A. Bianco, G. Ortaggi, M. Savino, *Bioorg. Med. Chem. Lett.* **2002**, *12*, 2527–2533; b) M. Franceschin, A. Alvino, G. Ortaggi, A. Bianco, *Tetrahedron Lett.* **2004**, *45*, 9015–9020; c) L. Rossetti, M. Franceschin, S. M. Schirripa, A. Bianco, G. Ortaggi, M. Savino, *Bioorg. Med. Chem. Lett.* **2005**, *15*, 413–420; d) A. Alvino, M. Franceschin, C. Cefaro, S. Borioni, G. Ortaggi, A. Bianco, *Tetrahedron* **2007**, *63*, 7858–7865; e) M. Franceschin, C. Lombardo, E. Pascucci, D. D'Ambrosio, E. Micheli, A. Bianco, G. Ortaggi, M. Savino, *Bioorg. Med. Chem.* **2008**, *16*, 2292–2304; f) E. Micheli, C. Lombardo, D. D'Ambrosio, M. Franceschin, S. Neidle, M. Savino, *Bioorg. Med. Chem. Lett.* **2009**, *19*, 3903–3908.

[26] a) J.-H. Fuhrhop, D. Fritsch, *Acc. Chem. Res.* **1986**, *19*, 130–137; b) G. Escamilla, G. Newkome, *Angew. Chem.* **1994**, *106*, 2013–2016; *Angew. Chem. Int. Ed. Engl.* **1994**, *33*, 1937–1940; c) J.-H. Fuhrhop, T. Wang, *Chem. Rev.* **2004**, *104*, 2901–2937.

[27] A. Geall, I. Blagbrough, *Tetrahedron* **2000**, *56*, 2449–2460.

[28] G. Schnurpfeil, J. Stark, D. Wöhrle, *Dyes Pigm.* **1995**, *27*, 339–350.

[29] a) F. Würthner, C. Thalacker, S. Diele, C. Tschierske, *Chem. Eur. J.* **2001**, *7*, 2245–2253; b) Z. Chen, U. Baumeister, C. Tschierske, F. Würthner, *Chem. Eur. J.* **2007**, *13*, 450–465; c) Z. Chen, V. Stepanenko, V. Dehm, P. Prins, L. Siebbeles, J. Seibt, P. Marquetand, V. Engel, F. Würthner, *Chem. Eur. J.* **2007**, *13*, 436–449.

[30] a) C. Hippius, I. van Stokkum, E. Zangrando, R. Williams, M. Wykes, D. Beljonne, F. Würthner, *J. Phys. Chem. C* **2008**, *112*, 14626–14638; b) J. Han, A. Shaller, W. Wang, A. Li, *J. Am. Chem. Soc.* **2008**, *130*, 6974–6982; c) E. Schwartz, V. Palermo, C. Finlayson, Y.-S. Huang, M. Otten, A. Liscio, S. Trapani, I. González-Valls, P. Brocorens, J. M. Cornelissen, K. Peneva, K. Müllen, F. Spano, A. Yartsev, S. Westenhoff, H. Friend, D. Beljonne, R. Nolte, P. Samorì, A. Rowan, *Chem. Eur. J.* **2009**, *15*, 2536–2547.

[31] Reproducible dimerization constants for all systems could be obtained only for the lowest energy band of the $S_0 \rightarrow S_1$ transition (520–530 nm).

[32] a) D. Aikens, S. Bunce, F. Onasch, R. Parker III, C. Hurwitz, S. Clemans, *Biophys. Chem.* **1983**, *17*, 67–74; b) H. Geneste, M. Hesse, *Chem. Unserer Zeit* **1998**, *32*, 206–218.

[33] Z.-R. Liu, R. Rill, *Anal. Biochem.* **1996**, *236*, 139–145.

[34] a) J. Suh, H.-J. Paik, B. Hwang, *Bioorg. Chem.* **1994**, *23*, 318–327; b) H.-J. Schneider, L. Tianjun, N. Lomadze, *Angew. Chem.* **2003**, *115*, 3668–3671; *Angew. Chem. Int. Ed.* **2003**, *42*, 3544–3546.

[35] R. Fink, J. Seibt, V. Engel, M. Renz, M. Kaupp, S. Lochbrunner, H.-M. Zhao, J. Pfister, F. Würthner, B. Engels, *J. Am. Chem. Soc.* **2008**, *130*, 12858–12859.

[36] a) H. Hansma, *J. Vac. Sci. Technol. B* **1996**, *14*, 1390–1394; b) J. Tamayo, R. Garacia, *Langmuir* **1996**, *12*, 4430–4435.

[37] D. Perrin, W. Armarego, *Purification of Laboratory Chemicals*, 2nd ed., Pergamon Press, Oxford, **1981**.
[38] J. Leonard, B. Lygo, J. Procter, *Praxis der Organischen Chemie*, Wiley-VCH, Weinheim, **1996**.
[39] M. Hesse, H. Meier, B. Zeeh, *Spektroskopische Methoden in der Organischen Chemie*, Thieme, Stuttgart, **2005**.
[40] a) J. Demas, G. Crosby, *J. Phys. Chem.* **1971**, *75*, 991–1024; b) J. Lakowicz, *Principles of Fluorescence Spectroscopy*, Kluwer Academic Plenum Publishers, New York, **1999**.

Received: October 14, 2009
Published online: February 8, 2010

